THE JOURNAL OF BIOLOGICAL CHEMISTRY
Vol. 277, No. 28, Issue of July 12, pp. 24949–24958, 2002
Printed in U.S.A.

Receptor-selective Effects of Endogenous RGS3 and RGS5 to Regulate Mitogen-activated Protein Kinase Activation in Rat Vascular Smooth Muscle Cells*

Received for publication, April 19, 2002, and in revised form, May 1, 2002
Published, JBC Papers in Press, May 2, 2002, DOI 10.1074/jbc.M203802200

Qin Wang‡, Min Liu‡, Bashar Mullah§, David P. Siderovski¶, and Richard R. Neubig‡‖**

From the ‡Departments of Pharmacology and ‖Internal Medicine/Hypertension, the University of Michigan, Ann Arbor, Michigan 48109-0632, §Applied Biosystems, Foster City, California 94404, and the ¶Department of Pharmacology, Lineberger Comprehensive Cancer Center and University of North Carolina Neuroscience Center, the University of North Carolina, Chapel Hill, North Carolina 27599-7365

Regulators of G protein signaling (RGS) proteins compose a highly diverse protein family best known for inhibition of G protein signaling by enhancing GTP hydrolysis by Gα subunits. Little is known about the function of endogenous RGS proteins. In this study, we used synthetic ribozymes targeted to RGS2, RGS3, RGS5, and RGS7 to assess their function. After demonstrating the specificity of *in vitro* cleavage by the RGS ribozymes, rat aorta smooth muscle cells were used for transient transfection with the RGS-specific ribozymes. RGS3 and RGS5 ribozymes differentially enhanced carbachol- and angiotensin II-induced MAP kinase activity, respectively, whereas RGS2 and RGS7 ribozymes had no effect. This enhancement was pertussis toxin-insensitive. Thus RGS3 is a negative modulator of muscarinic m3 receptor signaling, and RGS5 is a negative modulator of angiotensin AT1a receptor signaling through $G_{q/11}$. Also, RGS5 ribozyme enhanced angiotensin-stimulated inositol phosphate release. These results indicate the feasibility of using the ribozyme technology to determine the functional role of endogenous RGS proteins in signaling pathways and to define novel receptor-selective roles of endogenous RGS3 and RGS5 in modulating MAP kinase responses to either carbachol or angiotensin.

Heterotrimeric G protein-mediated receptor signaling pathways are important components of the complex biological processes controlling cellular function. These pathways involve the activation of Gα subunits by exchange of GDP for GTP, resulting in the dissociation of Gα from G$\beta\gamma$ subunits. Both subunits transduce signals to a variety of G protein effectors including adenylyl cyclase, voltage-sensitive Ca^{2+} and K^+ channels, phosphatidylinositol 3-kinase, phospholipases C-β and A2, cGMP phosphodiesterase, and indirectly MAP kinase[1] (1, 2). The regulator of G protein signaling (RGS) proteins makes up a highly diverse protein family best known to bind directly Gα subunits in their active GTP-bound state and stimulate GTP hydrolysis (GTPase-activating protein (GAP)), thus turning off G protein signaling (3–6).

Numerous studies of the specificity between RGS proteins and Gα subunits have been reported using biochemical, immunochemical, and functional methods. RGS proteins are GAPs for all Gα proteins (5–7). RGS2 is a strong GAP for $G\alpha_q$ (8), whereas RGS4 is a strong GAP for both $G\alpha_q$ and $G\alpha_i$ (9, 10). RGS7, -9, and -14 have marked preference for $G\alpha_o$ over other Gα subunits (10, 11). Less is known about RGS3 and RGS5. RGS5 is a member of RGS subfamily B that includes RGS1–5, -8, -16, and Gα interacting protein (12, 13) and has greatest sequence similarity to RGS4 and RGS16. RGS5 is highly expressed in heart, skeletal muscle, and thoracic aorta (14) and can bind to $G\alpha_{i1}$, $G\alpha_{i2}$, $G\alpha_{i3}$, $G\alpha_o$, and $G\alpha_q$ (15). RGS3 is a structurally distinct member of the RGS subfamily B with a unique long N-terminal domain. It has GAP activity for most $G\alpha_i$ family subunits and $G\alpha_q$ but not for $G\alpha_z$, $G\alpha_s$, or $G\alpha_{12}$ (16). It has also been shown to bind to $G\alpha_{11}$ (17).

Recent studies have identified receptor-specific effects of RGS protein action (18–20). In co-transfection studies of gonadotropin-releasing hormone receptor with different RGS cDNAs, only RGS3 expression suppressed gonadotropin-releasing hormone-induced IP_3 responses (18). In pancreatic acinar cells, microinjected RGS4 selectively inhibits calcium signals induced by muscarinic *versus* cholecystokinin receptors (19). An alternatively spliced N-terminal PDZ domain of RGS12 selectively binds to the C terminus of interleukin-8 receptor-B (20).

Even though these previous studies have provided evidence for RGS-Gα and RGS receptor specificity, the functional role of endogenous RGS proteins in cells and tissues is still not clear. A few studies on the function of endogenous RGS proteins are emerging. First, endogenous RGS proteins in rat superior cervical ganglion neurons tonically inhibit α_2-adrenergic receptor regulation of voltage-gated N-type calcium current, as determined with an RGS-insensitive $G\alpha_o$ subunit (21). Second, in an RGS9-1 knockout mouse, the rapid deactivation of transducin is lost, and the recovery of rod photoresponses is greatly slowed (22). RGS2 knockout mice exhibit an "anxious" behavioral phenotype and impaired immunity with reduced T cell proliferation and interleukin-2 production (23). Microinjection of anti-

* This work was supported by National Institutes of Health Grants GM 39561 (to R. R. N.), University of Michigan Biomedical Research Council grant (to Q. W.), and National Institutes of Health Grant GM 62338 (to D. P. S.). The costs of publication of this article were defrayed in part by the payment of page charges. This article must therefore be hereby marked "*advertisement*" in accordance with 18 U.S.C. Section 1734 solely to indicate this fact.

** To whom correspondence should be addressed: Dept. of Pharmacology, 1301 MSRB III, 1150 W. Medical Center Dr., Ann Arbor, MI 48109-0632. Tel.: 734-763-3650; Fax: 734-763-4450; E-mail: RNeubig@umich.edu.

[1] The abbreviations used are: MAP kinase, mitogen-activated protein kinase; AT1a, angiotensin 1a receptor; ERK, extracellular signal regulated kinase (p42/p44 MAPK); GAP, GTPase-activating protein; MAPK, MAP kinase; PTX, pertussis toxin; RGS, regulator of G protein signaling; RT-PCR, reverse transcription/PCR; RZ2, RGS2 ribozyme; RZ3, RGS3 ribozyme; RZ5, RGS5 ribozyme; RZ7, RGS7 ribozyme; a.u., arbitrary units; AngII, angiotensin II; IP*x*, inositol phosphates; RAOSMC, rat aorta smooth muscle cells.

TABLE I
RGS composition in A-10 cells

RT-PCR primers specific for the rat RGS subtypes (except for RGS3 and RGS7 sense primers that were from mouse sequences) were designed to anneal to the indicated sequences. The cDNA clones used for positive controls and the size of the expected product in RT-PCR analysis are also indicated. ND indicates not determined.

RGS	cDNA clone	Primer sequences 5′ to 3′	Expected product	mRNA	Protein
			bp		
2	Human	ATGTTCCTGGCTGTCCAGCAC TCATGTAGCATGGGGCTCCG	623	Yes	ND
3	Mouse	GAACTGGGTCGTAATGGAGGC CCTCTTTGCAAGCCTGGATTGC	456	Yes	Yes
4	Rat	ATGTGCAAAGGACTCGCTGGTC TTAGGCACACTGAGGGACTAG	615	No	ND
5	Mouse	GCCTGTGAGAATTACAAGAAG AGGGCGTAGATCCTTTTCTG	198	Yes	ND
6	Human	CTGGCCGTCCAAGATCTCAAG CAGCTTGTAGATGTGCTCCTG	198	No	ND
7	Human	CCAAGCCTCCTACAGAAGATG GGTAGGCACTAGATCTTATAAAG	584	Yes	No
9	Mouse	ATGACGATCCGACACCAAGGC CTTCTTCATGAGCATGTAAATG	1193	Yes	Yes
11	Human	GAGGCGTGTGAGGAGCTGC GAGCATGTAGATGTGCAGTTG	198	Yes	ND

bodies to RGS12 in primary culture of dorsal root ganglion neurons selectively slows the rate of desensitization of γ-aminobutyric acid, type B-mediated inhibition of tyrosine-phosphorylated N-type calcium channels (24). Finally, stable transfection of a full-length antisense RGS3 cDNA in NIH 3T3 cells abolishes the expression of endogenous RGS3 protein and significantly increases MAP kinase phosphorylation induced by endothelin-1 stimulation (17). Thus, only fragmentary information is available on the physiological function of endogenous RGS proteins in different cell systems.

Vascular smooth muscle participates in the normal control of vascular tone and pathological adaptation of arteries in hypertension and atherosclerosis (25) and is controlled by a number of G protein-coupled receptor pathways. The A-10 smooth muscle cell line established from rat thoracic aorta is an excellent model cell system for studying the role of RGS proteins in vascular smooth muscle signal transduction. It retains most of the spectrum of biological responses found in primary vascular smooth muscle cultures (26). A-10 cells express multiple receptors that regulate intracellular Ca^{2+} concentrations through phospholipase C, the Na^+/H^+ exchanger, and phosphorylation of growth factor receptor-binding protein-2 in regulation of MAP kinase activity (26–28). Thus A-10 cells contain a variety of endogenous receptor-G protein-effector signaling pathways that allow us to test the hypothesis that specific RGS proteins play important roles in specific signaling pathways in a living cell system.

To elucidate functional roles for specific endogenous RGS proteins, we have developed a ribozyme approach to inactivate specifically RGS protein at the mRNA level. In this study, we have inactivated the mRNAs encoding the RGS2, RGS3, RGS5, and RGS7 proteins in A-10 cells and primary culture of vascular smooth muscle cells. The results presented here define specific roles of RGS3 and RGS5 in inhibiting MAP kinase signaling by muscarinic and angiotensin receptors, respectively. This receptor-selective effect of RGS protein function provides new evidence for a unique targeting of RGS action to specific cellular responses.

EXPERIMENTAL PROCEDURES

Ribozyme Design and Synthesis—Chimeric DNA-RNA hammerhead ribozymes targeted against the RGS domains of rat RGS2, RGS3, RGS5, and RGS7 mRNA were chemically synthesized and modified by introducing two phosphorothioate linkages at the 3′-end using an Applied Biosystems 394 DNA/RNA synthesizer (Applied Biosystems Inc.) and then further purified by desilylating and desalting, as described previously (29). The structure and sequences of targeted sites on rat RGS ribozymes are shown in Fig. 2. Inactive control ribozymes were prepared in the same way but by scrambling the two flanking regions and introducing two point mutations in the catalytic core region (Fig. 2*A*) which have been shown previously (30) to prevent ribozyme cleavage activity.

In Vitro Ribozyme Cleavage—To generate *in vitro* RGS RNA transcripts as templates, pCR2.1 plasmids containing mouse RGS3 and RGS5 RGS cDNA were linearized with restriction enzymes (*Bam*HI and *Spe*I, respectively) and then transcribed with T7 RNA polymerase as recommended by the supplier (Promega, Madison, WI). To perform the *in vitro* cleavage experiment, the ribozyme and RGS RNA were denatured separately in 50 mM Tris-HCl, pH 8.5, at 90 °C for 30 s, then mixed in the presence of 20 mM $MgCl_2$ (total volume of 10 μl), and incubated at 50 or 37 °C for 1 h. Two pmol of template and 100 pmol of ribozyme were used. The reaction was stopped by the addition of 1 volume of stop solution consisting of 95% formamide and 60 mM Na-EDTA, pH 8.0, and subjected to denaturing mini-gel electrophoresis (5% polyacrylamide, 7 M urea) as described previously (31). Finally, the gel was stained with ethidium bromide and photographed.

Delivery of Ribozymes into Cells—The A-10 cell line, derived from the thoracic aorta of a DB1X embryonic rat, was obtained from the ATCC (catalog number CRL-1476) and grown in RPMI 1640 (Invitrogen) supplemented with 4 mM glutamine and 10% fetal bovine serum. The primary culture of rat smooth muscle cells (RAOSMC) derived from the tunica intima and inner layer of tunica media of healthy and fibrous plaque-free rat aorta were obtained from Cell Application, Inc. (San Diego, CA, catalog number R354-05) and grown in Rat Smooth Muscle Cell Growth Medium (Cell Application, Inc.). Both cells were maintained in a 37 °C incubator with 5% CO_2 in air atmosphere. A day before transfection, cells were plated in either 100-mm dishes (for analysis of protein suppression) or 6-well plates (for analysis of mRNA suppression, MAP kinase assay and IP*x* assay) and transfected at ~60–80% confluence with LipofectAMINE PLUS (Invitrogen) or Effectene transfection reagent (Qiagen, for MAP kinase and IP*x* assay only) according to the supplier's manual. The amount of RGS ribozyme transfected was 4 μg with 30 μl of LipofectAMINE for the 100-mm dish and 1 μg with 4 μl of LipofectAMINE for the 6-well plate, respectively. For Effectene, 0.5 μg of ribozyme and 12.5 μl of Effectene transfection reagent were used per well in 6-well plates. Sham transfection was done with either pcDNA3.1 plasmid or inactive ribozyme as indicated. The transfection efficiency, determined by transfection with the yellow fluorescent protein expression vector pEYFP (CLONTECH), was about 40–50% for either Effectene or LipofectAMINE methods in both cells.

Reverse Transcription-PCR (RT-PCR)—Total RNAs were prepared from either rat brain or A-10 cells with or without RGS-specific ribozyme transfection using RNeasy Mini kit (Qiagen) and then subjected to the RT-PCR with SuperScript™ One-Step™ RT-PCR System according to the supplier's manual (Invitrogen). A negative control was done using Ready-to-Go You-Prime First-Strand Beads (Amersham Biosciences) in which the first step of reverse transcription was omitted in the RT-PCR. Primer pairs generated from the RGS-coding region

were used to amplify each RGS as shown in Table I. Each pair of primers was first checked by amplifying RGS plasmid DNA to make sure that the correct size of the PCR product was achieved. For amplifying RGS2, RGS3, RGS7, and RGS9 in A-10 cells, total RNA of 200–400 ng was used with 0.3 μM primer and 1.2 mM $MgSO_4$ in a 25-μl volume. The reverse transcription was performed at 45 °C for 30 min and followed by PCR with 35–40 cycles at 95 °C for 30 s, 45 °C for 45 s, and 72 °C for 30 s. Different conditions were required for amplifying RGS5; total RNA of 400–800 ng was used with 8% Me_2SO and 1.8 mM $MgSO_4$ in a 25-μl volume, and then the RT-PCR was performed for 45 cycles at 95 °C for 30 s, 50 °C for 45 s, and 72 °C for 30 s. Similar conditions were used for amplifying RGS in RAOSMC by RT-PCR. For amplifying muscarinic receptor mRNA, subtype-specific primers for rat muscarinic receptors were designed as follows: m1, sense 5′-GAACACCTCAGTGCC-3′, antisense 5′-AGAGCTGCCCTTCGG-3′ (product 428 bp); m2, sense 5′-GGCTTGGCTATTACCAGTCC-3′, antisense 5′-GAGGATGAAGGAAAGGAC-3′ (product 432 bp); m3, sense 5′-CAACCTCGCCTTTGTTTCC-3′, antisense 5′-GGACAAAGGAGATGACCC-3′ (product 569 bp); m4, sense 5′CTTCACGCCTGTCAATGG 3′, antisense 5′-CTCTTGCCCACCACAAAC-3′ (product 422 bp); and m5, sense 5′-GGAAGGGGAGTCTTACAATG-3′, antisense 5′-GGAACTGGATCTGGCACTC-3′(product 556 bp). For RT-PCR of muscarinic receptors, 50 ng of total RNA from either rat brain or A-10 cells was amplified at 95 °C for 30 s, 50 °C for 45 s, and 72 °C for 40 s for 30 cycles in a 12.5-μl volume. Elongation factor 1α was amplified under identical condition as an internal control. The RT-PCR products were electrophoresed on a 1.8% agarose gel, stained with ethidium bromide stimulated with a Kodak ImageStation, and photographed. The intensity of the bands was quantified by densitometry analysis using the Kodak One-dimensional 3.5 software.

Western Blot for RGS3 Protein—Of the RGS proteins detected at the mRNA level in A-10 cells (RGS2, -3, -5, and -7), only RGS3, -7, and -9 antibodies were useful for Western blotting. Whole cell lysates were prepared from A-10 cells transfected with or without RGS ribozyme by suspending them in RIPA lysis buffer containing 1× phosphate-buffered saline, 1% Igepal CA-630 (Sigma), 0.5% sodium deoxycholate, 0.1% SDS with fresh addition of 0.15–0.3 TIU/ml aprotinin (Sigma), 1 mM sodium orthovanadate, 1 mM benzamidine, 1 μg/ml pepstatin, and 2 μg/ml leupeptin. Cells were passed 10 times through a 21-gauge needle; 10 μg/ml phenylmethylsulfonyl fluoride was added, and the mixture was incubated for another 1 h on ice and finally centrifuged at 10,000 × *g* for 10 min. The supernatant was saved as total cell lysate. Protein (60–100 μg) was subjected to SDS-PAGE on an 8% mini-gel and transferred to Immobilon™-P transfer membrane. The membrane was blocked with 3% milk in TBS (10 mM Tris-HCl, pH 8.0, 150 mM NaCl) without Tween 20 for 1 h and incubated with 1:200 anti-RGS3 antibody (Santa Cruz Biotechnology, sc-9304) overnight in the cold room. For screening RGS7 and RGS9 proteins, antibodies kindly supplied by Drs. Theodore Wensel (Baylor College of Medicine, Houston, TX) and Vladlen Slepak (University of Miami School of Medicine, FL) were used at 1:1,000 to 1:2,000 dilution for 1 h at room temperature. After three consecutive washes with TBS plus 0.05% Tween 20 (10 min for each), the membrane was incubated with 1:10,000 secondary antibody (anti-rabbit horseradish peroxidase linked $F(ab')_2$ fragment from donkey, Amersham Biosciences, catalog number NA 9340) for 1 h at room temperature. Prestained SDS-PAGE protein standards (Bio-Rad, catalog number 161-0309) were used to determine the size of detected proteins. For RGS3 samples, the blots were re-blotted with anti-G protein β-subunit antibody (Santa Cruz Biotechnology, sc-378) at 1:20,000 dilution after stripping as an internal control for the determination of protein loading. Proteins were visualized by chemiluminescence with SuperSignal West Dura (Pierce). The intensity of bands was quantified by densitometry analysis of films in the linear range of exposure using a Hewlett-Packard ScanJet scanner.

MAP Kinase Assay—A day before transfection, cells were plated into 6-well plates and transfected with either inactive or RGS-specific ribozymes with the Effectene transfection reagent (Qiagen). Thirty hours after transfection, cells were put into serum-free medium and then at 72 h post-transfection were washed with phosphate-buffered saline and stimulated with the appropriate agonist for 5 min, and finally harvested by addition of 250 μl of Stopping Buffer containing 1× Protein Loading Buffer with 50 mM dithiothreitol, 1 mM sodium orthovanadate, 10 mM sodium fluoride, 0.15–0.3 TIU/ml aprotinin (Sigma), 2 μg/ml leupeptin, and 1 mM EDTA, pH 8.0. For RAOSMC, cells were starved for 48 h and lysed with 100 μl/well 1× SDS Sample Buffer containing 62.5 mM Tris-HCl, pH 6.8, 2% SDS, 10% glycerol, 50 mM dithiothreitol, 0.01% bromphenol blue and immediately scraped off the plate. Then samples were heated at 95 °C for 5 min and cooled on ice. Finally, the lysates were subjected to 12% SDS-PAGE and transferred to Immobilon™-P transfer membrane for Western blotting. For A-10 cells, the blot was first probed with phospho-ERK antibody (1:500, Santa Cruz Biotechnology, sc-7383) to measure the activated phospho-ERK and visualized by chemiluminescence with SuperSignal West Dura (Pierce). Generally, only a single band at 42 kDa corresponding to phospho-ERK2 was observed in the A-10 cells. Some experiments showed a faint signal at 44 kDa corresponding to ERK1, but only the ERK2 results could be analyzed. The same blot was stripped and re-blotted with anti-ERK-2 which is reactive with ERK2 p42 and to a lesser extent with ERK1 p44 (1:1000, Santa Cruz Biotechnology, sc-153) to measure total ERK2 levels. MAP kinase activity was expressed as normalized arbitrary units (a.u.) of phosphorylated p42 MAP kinase (ERK2) over total ERK2 by densitometry analysis of films in the linear range of exposure using a Hewlett-Packard ScanJet scanner. For RAOSMC, the blot was first probed with Phospho-p44/42 MAPK (Thr-202/Tyr-204) E10 monoclonal antibody (1:1000, Cell Signaling Technology, catalog number 9106) to measure the activated phospho-ERK and visualized by chemiluminescence with SuperSignal (Pierce). Both p44 and p42 bands corresponding to phospho-ERK1/2 were observed in RAOSMC cells. The same blot was stripped and re-blotted with anti-ERK-2 (1:1000, Santa Cruz Biotechnology, sc-153) to measure total ERK levels. MAP kinase activity was expressed as normalized a.u. of phosphorylated p42/44 ERK over total ERK by densitometry analysis of films in the linear range of exposure using a Hewlett-Packard ScanJet scanner. Statistical analysis was done by using one- and two-way analysis of variance in Prism (GraphPad software, version 3.01) with Tukey's Multiple Comparison post-test to identify specific effects of the ribozymes.

Phosphoinositide Production—Measurment of inositol phosphates (IP*x* including inositol monophosphate, inositol bisphosphate, and inositol triphosphates) was done as described previously (32, 33). Briefly, RAOSMC cells were transfected with ribozymes as done for the MAP kinase assay. At 48 h post-transfection, cells were incubated with [^{3}H]myoinositol (10 μCi/ml/dish) for another 24 h at 37 °C in Dulbecco's modified Eagle's medium without inositol. Labeling was terminated by aspirating the medium and rinsing cells with oxygenated reaction buffer containing 142 mM NaCl, 30 mM Hepes buffer, pH 7.4, 5.6 mM KCl, 3.6 mM $NaHCO_3$, 2.2 mM $CaCl_2$, 1.0 mM $MgCl_2$, 10 mM LiCl, and 1 mg/ml D-glucose. The stimulation of IP*x* production was initiated by incubating cells with different concentrations of AngII in 0.5 ml of reaction buffer for 30 min at 37 °C. Then the reaction was stopped by adding 0.5 ml of ice-cold 20% trichloroacetic acid, and samples were kept on ice for another 30 min. Cells were scraped, and precipitates were pelleted (4100 × *g*, 20 min). The trichloroacetic acid-soluble fraction was transferred to a new tube, extracted with water-saturated diethyl ether three times, and then neutralized with $NaHCO_3$. Finally, IP*x* was isolated by adsorption to 0.5 ml of 50% (w/w) Dowex AG 1-X8 formate resin slurry and rinsed with unlabeled 5 mM myoinositol three times, followed by elution with 1 ml of 1.2 M ammonium formate and 0.1 M formic acid. The elutes were counted by liquid scintillation counter in 10 ml of ScintiVerse.

Whole Cell [^{125}I]AngII Binding Assay—A-10 or RAOSMC cells were transfected using the same conditions as for the MAPK assays and rinsed with 1 ml of assay buffer containing 0.1% bovine serum albumin (Sigma catalog number A-6003) and 0.1 mg/ml bacitracin in Opti-MEM medium. Then cells were incubated with 100 pM [^{125}I-Tyr^4]angiotensin II (human, 2200 Ci/mmol, PerkinElmer Life Sciences, catalog number NEX105) in the assay buffer for 1 h at room temperature. For nonspecific binding, separate dishes were incubated with the same hot buffer plus 10 μM saralasin (Sigma catalog number A-2275). After incubation, cells were washed three times with assay buffer and precipitated with ice-cold 5% trichloroacetic acid for another 30 min in the cold room. Finally, the supernatant was aspirated and counted by liquid scintillation counter in 10 ml of ScintiVerse. Nonspecific binding represented ~0.3% of total binding.

RESULTS

Expression of RGS in A-10 Cells—Consistent with the known variety of endogenous receptor-G protein-effector pathways in A-10 cells, we have identified a number of RGS proteins that are expressed at both the mRNA and the protein levels in these cells. Previous studies have shown that RGS2, -3, and -10–12 and Gα interacting protein mRNA are present in primary cultures of rat vascular smooth muscle cells (34) and RGS1, -3–7, -9, -12, -14, and -16 are detectable in cardiomyocytes (35). Accordingly, we tested eight RGS genes for expression in A-10

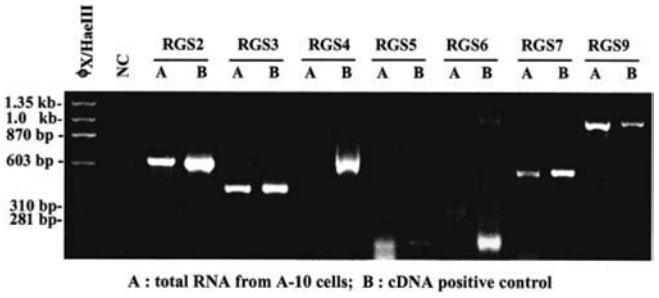

FIG. 1. **Expression of RGS mRNAs in A-10 cells.** Total RNA prepared from A-10 cells was subjected to RT-PCR (*lane A*) using RGS-specific primers (Table I) that were tested by amplifying RGS cDNA plasmids (*lane B*) as a positive control. The PCR products were separated on a 1.8% agarose gel, stained with ethidium bromide, and photographed. The expected sizes of PCR products are shown in Table I. *NC* indicates the negative control in which the reverse transcriptase was omitted before PCR amplification with RGS3 primers.

cells by RT-PCR. Five (RGS2, -3, -5, -7, and -9) of the eight tested RGSs were detected strongly at the mRNA level by RT-PCR (Fig. 1). RGS11 was weakly detected (data not shown), and RGS4 and RGS6 were not detectable. Positive control cDNA clones for all eight were readily amplified indicating correct choice of primers. At the protein level, only a few anti-RGS antibodies were tested due to the limited availability of good quality anti-RGS-specific antibodies. An RGS3 antibody detected a doublet at 60 kDa in A-10 cells consistent with the predicted size of 61.5 kDa for mouse RGS3 (GenBank™ accession number AF215670). RGS9 antibody detected a strong doublet at ~72 kDa consistent with the 77-kDa predicted molecular mass for the long splice variant of RGS9 (data not shown). RGS7 antibody did not detect a signal in A-10 cells under current conditions but did detect a very strong band at ~55 kDa in a rat brain lysate positive control (data not shown). Thus RGS7 while showing abundant mRNA levels did not show detectable protein expression. Thus, we were able to confirm protein expression of RGS3 and RGS9 but not RGS7, whereas RGS2 and RGS5 could not be tested due to the unavailability of antibodies. This varied complement of RGS expression in A-10 cells allowed us to test directly the hypothesis that endogenous RGS proteins contribute to the specificity and regulation of receptor signaling in vascular smooth muscle.

Design and Synthesis of Rat RGS-specific DNA-RNA Chimeric Hammerhead Ribozymes—To determine the functional role of the endogenous RGS proteins, we designed hammerhead ribozymes that were targeted to a GUC sequence encoding the RGS domain within RGS2, -3, -5, and -7 mRNA. The "GUC" cleavage sites in the RGS domain were chosen because the RGS domain is a known functional region of RGS proteins. Several GUC sequences were present in each RGS mRNA, so selection of gene-specific target sites was done by manually searching for a unique nucleotide composition of the flanking region as shown in Fig. 2*B*. Because this study was ultimately aimed at using ribozymes in cell systems, the RGS ribozymes were chemically synthesized as a chimeric DNA-RNA construct to improve their resistance to intracellular endonucleases. The chimeric DNA-RNA ribozyme (Fig. 2*A*) consisted of a catalytic core containing ribonucleotides (in *lowercase letters*) and flanking sequences containing deoxyribonucleotides (in *capital letters*), which hybridize specifically to the targeted RGS mRNA transcript by Watson-Crick base pairing. In addition, two phosphorothioate linkages were added to the 3′-end of the ribozyme to improve the stability and cellular delivery of the ribozymes as shown previously (29).

Catalytic Activity of RGS Ribozyme in Vitro—To confirm that the RGS ribozymes were capable of cleaving the targeted RNA,

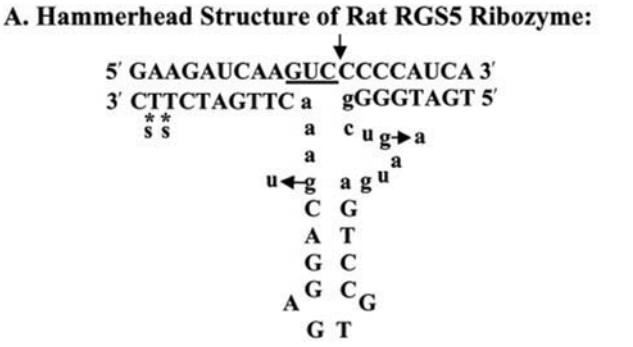

C. *In vitro* cleavage of RGS5 ribozyme:

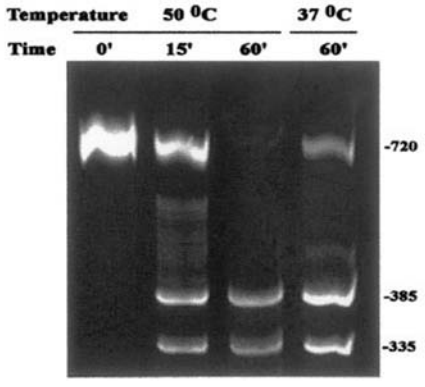

FIG. 2. **Sequence, structure, and *in vitro* cleavage of rat RGS-specific hammerhead ribozymes.** *A*, the targeted RGS5 mRNA transcript is shown in the 5′ to 3′ direction (*upper sequence*). The constructed DNA-RNA chimeric hammerhead ribozyme is shown in the complementary 3′ to 5′ direction (*lower sequence*). The targeted GUC trinucleotide in the RGS mRNA is *underlined*, and the cleavage site is indicated by the *arrow*. The ribonucleotides of the ribozyme required for catalytic activity in the core region are shown in *lowercase letters*, and the complementary flanking regions of deoxyribonucleotides are shown in *capital letters*. The positions of the two phosphorothioate linkages at the 3′-terminal region of the ribozyme, added to enhance stability, are indicated by *asterisks*. The nucleotides and *arrows* in the catalytic core region indicate changes to generate the inactive ribozymes. *B* shows the targeting site in the RGS domain for the four rat RGS-specific ribozymes. *C*, *in vitro* cleavage of RGS5 mRNA transcripts by the RGS5 ribozyme. The chemically synthesized RGS5 ribozyme and RGS5 mRNA transcript (50:1 ratio) were incubated together for 15 or 60 min and then the cleavage products were separated on a 5% polyacrylamide, 7 M urea gel, visualized by ethidium bromide staining, and photographed. The full-length RGS5 transcripts (720 bp) were cleaved into two small fragments (385 and 335 bp) at 50 °C. The RGS5 ribozyme also showed good cleavage activity in 60 min at physiological temperatures (37 °C).

the catalytic activity of RGS ribozymes was examined using RGS RNA transcribed *in vitro*. As shown in Fig. 2*C*, RGS5 RNA synthesized from a mouse RGS5 cDNA clone generated a product of 720 bases that includes the entire 546 bases of RGS5 coding region sequence, 77 bases of 3′-untranslated sequence,

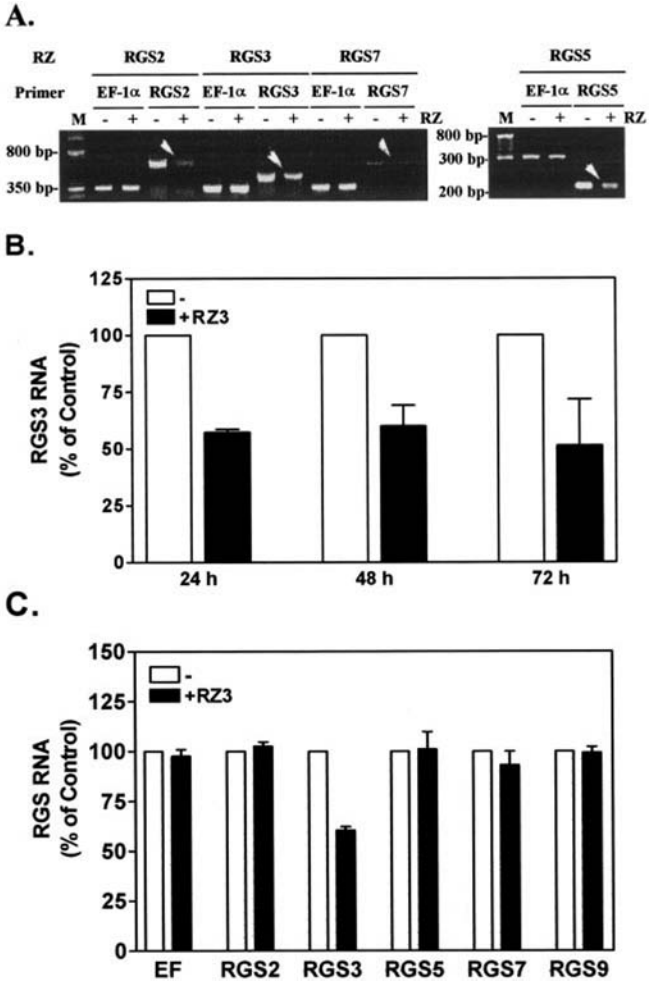

FIG. 3. **Suppression of endogenous RGS mRNA expression in RGS ribozyme-transfected A-10 cells.** *A*, effect of RGS ribozyme cleavage on RGS mRNA level in A-10 cells. Total RNAs were prepared from plasmid control (−) and RGS ribozyme-transfected (+) A-10 cells at 48 h after transfection, and the levels of RGS mRNA transcripts were quantified by RT-PCR analysis. RT-PCR was done under the same PCR conditions for RGS3, RGS2, RGS7, and RGS9. RGS5 required a modified RT-PCR protocol (see "Experimental Procedures"). A control mRNA, elongation factor 1α (*EF-1α*), was tested using the same RT-PCR conditions as used for the RGS being studied. PCR products were separated on a 1.8% agarose gel and visualized by ethidium bromide staining. The expected sizes of PCR product are indicated in Table I. EF-1α in each set showed very similar intensity with or without RGS ribozyme treatment, whereas the RGS mRNA was suppressed only in the cells treated with that RGS-specific ribozyme (*arrowheads*). *B*, time course of RGS3 mRNA suppression by RGS3 ribozyme treatment in A-10 cells. Total RNA was prepared from control (pCDNA3.1, −) and active RGS3 ribozyme-transfected (+RZ3) A-10 cells at 24, 48, and 72 h post-transfection, and the levels of RGS3 mRNA were quantified by RT-PCR analysis. Data represent mean ± S.E. from three experiments. *C*, gene specificity of RGS3 ribozyme suppression at mRNA level in A-10 cells. Total RNA was prepared from control (pCDNA3.1, −) and RGS3 ribozyme-transfected A-10 cells (+RZ3) at 48 h post-transfection, and the levels of different RGS mRNA transcript were quantified by RT-PCR analysis. Data are mean ± S.E. of three determinations.

and 71 bases of 5′- and 26 bases of 3′-multicloning regions of pCR2.1 vector. Mouse RGS5 is 94% identical to the rat RGS5 cDNA at the nucleotide level and 100% identical over the RGS5 ribozyme flanking regions. Addition of the RGS5 ribozyme to the RGS5 RNA transcript generated two expected fragments of 385 and 335 bases corresponding to cleavage at the targeted GUC site. Thus the ribozyme-mediated cleavage of the RGS5 RNA transcript was site-specific. Furthermore, over 90% of the template was cleaved in 1 h at 37 °C indicating that this RGS5 ribozyme is capable of disrupting the RGS5 mRNA at a physiological temperature. Similar results were obtained with the RGS3 ribozyme (not shown). These results indicate that the designed RGS ribozymes are capable of efficiently cleaving the targeted mRNA in a site-specific fashion.

Effect of RGS Ribozymes on RGS mRNA in Cells—To examine the activity of the RGS ribozymes in intact cells, they were introduced into rat A-10 cells by transient transfection with LipofectAMINE PLUS. At 48 h post-transfection, total RNA was extracted from cells transfected with or without the designated RGS ribozyme, and the level of RGS mRNA was determined by RT-PCR. As shown in Fig. 3*A*, the level of each RGS mRNA (*i.e.* RGS2, -3, -5, and -7) was decreased by its own RGS-specific ribozyme compared with the control without ribozyme (*i.e.* sham-transfected with pcDNA3.1 vector). The control elongation factor 1α transcript was unaffected by ribozymes in each case. To test the time course of ribozyme effects, RGS3 mRNA expression was determined at 24, 48, and 72 h post-transfection with RGS3 ribozyme. The level of RGS3 mRNA was reduced to 57 ± 1.4, 60 ± 9.1, and 51 ± 20% (n = 3) of the control level determined without RGS3 ribozyme transfection (Fig. 3*B*). To establish that the specificity of RNA cleavage was maintained upon delivery of the RGS ribozyme into cells, we examined the effect of transfection with RGS3 ribozyme on the level of other RGS mRNAs. As shown in Fig. 3*C*, transfection of A-10 cells with RGS3 ribozyme did not reduce the level of the elongation factor 1α mRNA or that of any of the other RGS mRNAs (RGS2, RGS5, RGS7, and RGS9) tested. In these same cells, the level of the RGS3 mRNA was reduced to 60 ± 1.9% (n = 3) of its control value. Transfection of an inactive control RGS3 ribozyme (*RZ3m*, Fig. 2) did not reduce the level of RGS3 RNA (data not shown). These data clearly demonstrate the cleavage activity and specificity of the synthetic hammerhead RGS ribozymes for the targeted RGS RNA when delivered into intact cells by transfection. Given the fact that the transfection efficiency in A-10 cells determined from yellow fluorescent protein expression was about 40–50%, the 40–50% reduction of RNA level most likely represents a nearly complete suppression in the transfected cell population.

Effect of RGS3 Ribozyme on the Level of RGS3 Protein in A-10 Cells—Next, we investigated whether the suppression in RGS3 RNA was paralleled by a similar reduction in the amount of RGS3 protein in cells transfected with the RGS3 ribozyme. For this purpose, A-10 cells were transfected with either no ribozyme (*i.e.* sham-transfected with pCDNA3.1 vector) or RGS3 ribozyme and harvested at 72 h post-transfection. Whole cell lysates were prepared from these cells and evaluated by immunoblotting with anti-RGS3 antibody. Fig. 4*A* shows a representative immunoblot probed with anti-RGS3 antibody and then probed with an anti-Gβ antibody as a loading control. Gβ antibody alone showed a single band at 35 kDa, and the amount of G protein β subunit was not changed by RGS3 ribozyme transfection. The RGS3 antibody detected a doublet band of ~60 kDa in control cells that was clearly reduced in the cells transfected with the RGS3 ribozyme. Fig. 4*B* shows a quantitative analysis of these results in which the relative amounts of RGS3 protein and Gβ were quantified and expressed as a percentage of the control level. RGS3 protein was suppressed to 45 ± 1% of the control value in ribozyme-treated cells, whereas the level of Gβ in ribozyme-treated cells was 107 ± 6% of control. Thus the RGS3 ribozyme suppresses RGS3 protein levels as well as mRNA levels.

Differential Effects of RGS3 and RGS5 Ribozymes in Enhancing Carbachol- and Angiotensin II-stimulated MAP Kinase Activity—It was previously shown that RGS3 and other members of the RGS family can inhibit G protein-stimulated MAP kinase activation when transfected into cells either tran-

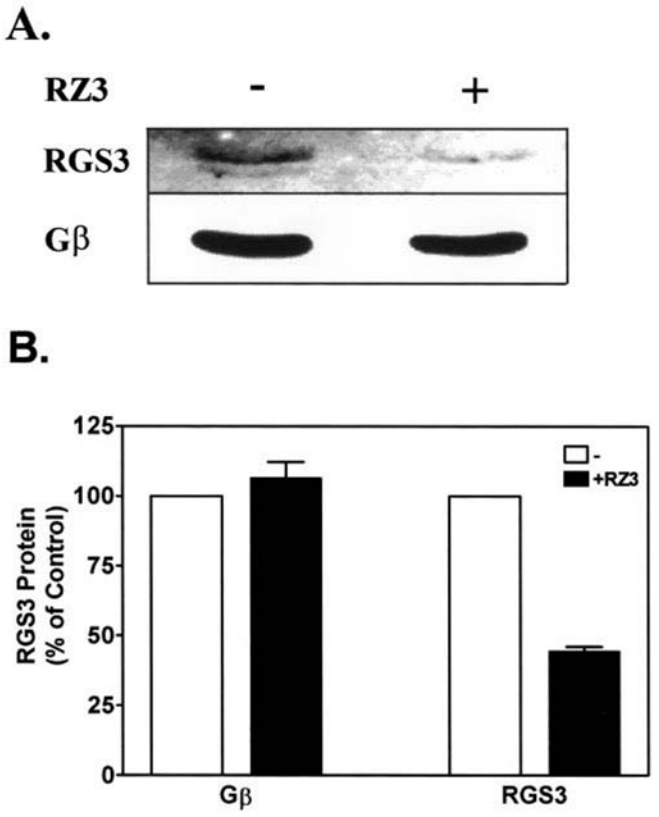

FIG. 4. **Suppression of endogenous RGS3 protein expression in RGS3 ribozyme-transfected A-10 cells.** *A*, Western blot of RGS3 protein. Whole cell lysates were prepared from A-10 cells 72 h after transfection with (+RZ3) or without (pCDNA3.1, −) RGS3 ribozyme and resolved on 8% SDS-PAGE for Western blot analysis as described under "Experimental Procedures." The anti-RGS3 antibody detected a doublet of about 60 kDa and anti-G protein β-subunit antibody (Gβ) was used as an internal control for the determination of equal protein loading. *B*, quantitative analysis of RGS3 and Gβ expression in ribozyme-treated samples, presented as mean ± S.E. of percent of control from three experiments similar to that shown in *A*.

siently (36, 37) or in a stable manner (17). Because overexpression can elicit effects that do not occur at normal protein levels, we wanted to determine whether any endogenous RGSs influence MAP kinase activity in A-10 cells stimulated by an endogenous receptor. A-10 cells were transiently transfected with inactive RGS3 ribozyme or a panel of active RGS ribozymes, and then carbachol-induced activation of MAP kinase was determined by Western blotting with a phospho-specific ERK antibody (Fig. 5, *A* and *C*). ERK phosphorylation was expressed as a ratio (normalized arbitrary units) of phosphorylated p42 MAP kinase (ERK2) divided by total ERK2 as determined by densitometry analysis. Through endogenous receptors, carbachol alone caused only a 31% increase in phospho-ERK levels (96 *versus* 65 a.u.). This was blocked by 1 μM atropine indicating a muscarinic cholinergic mechanism (data not shown). None of the RGS ribozymes caused a significant increase in phospho-ERK levels in the absence of agonist (Fig. 5*C*). Only the RGS3 ribozyme significantly enhanced carbachol-stimulated MAP kinase activity (Fig. 5*C*, *Carb/RZ3*, 139 ± 9, *versus Carb/RZ3m*, 96 ± 8 a.u., $p < 0.01$). This represents a 43% increase compared with the inactive control RGS3 ribozyme (*RZ3m*). The other RGS ribozymes had no effect on carbachol-stimulated MAP kinase activity. Thus endogenous RGS3 appears to be a negative modulator of MAP kinase activity in muscarinic receptor signaling in A-10 cells.

Next, we investigated whether any endogenous RGSs would influence MAP kinase activity stimulated by angiotensin in A-10 cells. Because the AT1a receptor is not expressed in A-10 cells, we co-transfected the rat AT1a receptor together with the same panel of RGS-specific ribozymes used above or the inactive RGS5 ribozyme (RZ5m) as a control. Angiotensin II (AngII) induced phosphorylation and activation of MAP kinase was again determined by Western blotting with the phospho-ERK antibody at 72 h post-transfection. As with carbachol, AngII alone caused only a small increase of 28% in phospho-ERK levels compared with nonstimulated controls (87 ± 7 *versus* 67 ± 2, Fig. 5, *B* and *D*). Surprisingly, the RGS5 ribozyme but not the RGS3 ribozyme enhanced AngII-stimulated MAP kinase activity. RGS5 ribozyme caused a 64% increase (Fig. 5*D*, *AngII/RZ5*, 141 ± 14, *versus AngII/RZm5*, 86 ± 7, $p < 0.005$) compared with AngII with the inactive RGS5 ribozyme (*RZ5m*). The other RGS ribozymes had no effect on AngII-stimulated MAP kinase activity. To rule out an effect of the RGS5 ribozyme on receptor expression in A-10 cells, ^{125}I-AngII binding to intact cells was measured under the transfection conditions identical to those for MAPK assays. Results from the triplicate measurements expressed as a percentage of the RZ5m data were as follows: RZ5m 100%, RZ5 108 ± 0.008%, and RZ3 108 ± 0.02%. So ribozyme transfection did not alter signaling via an effect on receptor expression. These data demonstrate a differential effect of endogenous RGS3 and RGS5 on MAP kinase activity induced by endogenous muscarinic receptor and exogenous AT1a receptors in A-10 cells. We thus provide novel evidence of receptor specificity of the effects of endogenous RGS3 and RGS5 protein in this vascular smooth muscle cell line.

PTX Insensitivity of RGS3 and RGS5 Ribozyme-enhanced MAP Kinase Activity—The RGS specificity observed in Fig. 5 could result from different G proteins mediating receptor coupling to MAP kinase activation (*i.e.* G_q or G_i family). We therefore wanted to determine whether the enhancement of MAP kinase activity by RGS3 and RGS5 ribozymes was sensitive to pertussis toxin (PTX). Accordingly, A-10 cells were transfected with active RGS3 or RGS5 ribozyme or the corresponding inactive control ribozyme and then treated with or without pertussis toxin overnight. Agonist-induced MAP kinase activity was measured with or without carbachol or AngII stimulation. Both carbachol (Fig. 6*A*) and AngII (Fig. 6*B*) still stimulated MAP kinase activity, and this stimulation was still enhanced by the RGS3 ribozyme or RGS5 ribozyme, respectively, even after PTX pretreatment. Maximal values for phospho-ERK with agonist stimulation plus RGS ribozyme were 186 ± 7 (n = 5) for Carb/RZ3 and 162 ± 2 (n = 3) for AngII/RZ5. The maximal agonist/RZ effects with PTX were similar to those without PTX (201 ± 10, n = 3, for Carb/RZ3; 154 ± 19, n = 6, for AngII/RZ5). The inability of PTX to reduce ribozyme-enhanced MAP kinase activity indicates that both carbachol and AngII responses are mediated through a non-$G_{i/o}$ signaling mechanism, most likely through a $G_{q/11}$ family G protein. Thus the differences between effects of RGS3 and RGS5 protein on carbachol and AngII stimulation do not appear to result from differential G protein coupling (G_i *versus* G_q), as both receptor systems are likely using G_q family proteins (see "Discussion").

Characterization of Muscarinic Receptor Subtypes in A-10 Cells—There are five subtypes (m1, m2, m3, m4, and m5) of muscarinic receptors with the "odd-numbered" muscarinic receptor (m1, m3, and m5) subtypes typically coupled via the PTX-insensitive $G_{q/11}$ family, whereas the "even-numbered" members (m2 and m4) generally activate PTX-sensitive G_i/G_o (38). RGS3 ribozyme enhancement of carbachol-stimulated phospho-ERK activity was not abolished by PTX pretreatment (Fig. 6*A*) suggesting the involvement of muscarinic receptor subtypes m1, m3, or m5 in this signaling pathway. To charac-

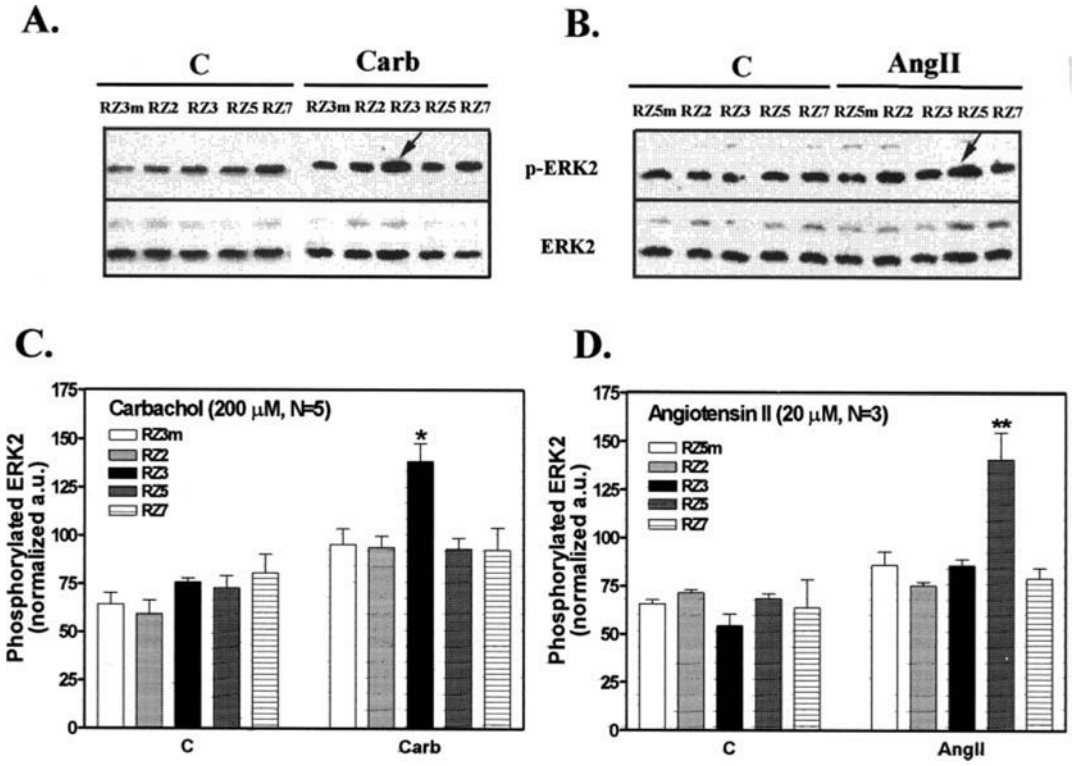

FIG. 5. **Differential effects of RGS3 and RGS5 ribozymes in enhancing carbachol- and angiotensin II-stimulated MAP kinase activity.** *A* and *C*, A-10 cells were transfected with the inactive RGS3 ribozyme (RZ3m) or with the panel of RGS-specific ribozymes (RZ2, RZ3, RZ5, or RZ7). After ~30 h, serum was removed from the medium and at 72 h post-transfection, A-10 cells were stimulated with 200 μM carbachol for 5 min, harvested, and subjected to 12% SDS-PAGE for MAP kinase analysis by Western blot using ERK-2 and phospho-ERK antibodies as described under "Experimental Procedures." *A* is a representative Western blot and the *C* shows the mean ± S.E. of five independent experiments. The *asterisk* indicates that RGS3 ribozyme produced a statistically significant ($p < 0.01$) enhancement of carbachol-stimulated MAP kinase activity (*Carb*, *black bar*) compared with carbachol plus the inactive RGS3 ribozyme (*Carb*, −, *white bar*). *B* and *D*, A-10 cells were co-transfected with the AT1a receptor plasmid plus either the inactive RGS5 ribozyme (*RZ5m*) or the same panel of four RGS-specific ribozymes and then serum-starved for ~40 h prior to stimulation with 20 μM AngII for 5 min at 72 h post-transfection. Cells were harvested, subjected to SDS-PAGE, and analyzed by Western blotting. *B* is a representative Western blot, and the *D* shows mean ± S.E. values from three independent experiments. ** indicates a p value <0.003.

terize further the muscarinic receptor subtypes in A-10 cells, specific primers were designed to amplify each muscarinic receptor subtype by RT-PCR from total RNA prepared from rat brain (as positive control) or from A-10 cells. As shown in Fig. 7, all five subtypes were easily detected in rat brain mRNA, but only m3 was strongly detected in A-10 cells. m4 was detectable, and m1 showed a very weak band. Thus an endogenous m3 subtype of muscarinic receptor seems to be involved in RGS3 ribozyme-enhanced MAP kinase activation.

RGS5 Ribozyme Enhances Angiotensin II-stimulated MAP Kinase and IPx Accumulation through Endogenous AT1a Receptors in Primary Cultures of Aortic Smooth Muscle—In an effort to show a more robust effect of RGS knockdown on Erk activation and to assess effects on an endogenous AT1aR, we turned to primary cultures of RAOSMC. These cells express high levels of endogenous angiotensin AT1a receptor. Furthermore, the mRNAs for RGS2–7 and -11 but not -9 were detectable by RT-PCR (data not shown). As shown in Fig. 8, 1 nM AngII produces a significant stimulation of ERK1/2 phosphorylation (3.3 ± 0.5- and 2.9 ± 0.8-fold for the control inactive ribozymes RZ5m and RZ3m). Transient transfection of the active RGS5 ribozyme (RZ5) dramatically increased AngII-stimulated phosphorylation of ERK1/2 (to 6.2 ± 1.9-fold). On the other hand, the RGS3 ribozyme (RZ3) had no effect (AngII stimulation of 3.2 ± 1.4-fold). Preliminary studies also showed no effect of RGS2 or RGS7 ribozymes in RAOSMC cells. With higher doses of AngII stimulation (*e.g.* 10 nM), there was no difference between the different transfected ribozyme in enhancing ERK1/2 activation (data not shown). This effect to enhance the sensitivity of receptor responses but not the maximum effect is similar to that seen in the sst2-deleted strains of *Saccharomyces cerevisiae* (39) and for adrenergic regulation of ion channels by RGS-resistant $G\alpha_o$ subunits (21). These results show a more robust effect of RGS5 ribozyme and confirm the lack of effect of RGS3 ribozyme on AngII-stimulated phosphorylation of ERK. To rule out that the effects of RGS5-specific ribozyme on ERK activation is due to an increase in receptor expression in RAOSMC cells, ^{125}I-AngII whole cell binding was measured. Results expressed as a percentage of RZ5m from the average of duplicates were as follows: RZ5m 100%, RZ3m 101 ± 0.02%, RZ2 104 ± 0.04%, RZ3 106 ± 0.03%, RZ5 106 ± 0.004%, and RZ7 106 ± 0.02%. Because the same specificity is seen in A-10 cells with transfected AT1aR and for the endogenously expressed AT1aR in primary cultures, it is likely that RGS5 plays an important role in regulation of angiotensin signaling in vascular smooth muscle *in vivo*.

To look at the effects of endogenous RGS on upstream components of angiotensin signaling pathways, we assessed inositol phosphates (IP*x*) release in RAOSMC. As shown in Fig. 9, transient transfection of RGS5 ribozyme (*RZ5*) enhanced IP*x* accumulation by the lowest doses (1–3 nM) of AngII compared with the control cells transfected with inactive ribozyme (*RZ5m*). Also, the RGS3 ribozyme had no effect on AngII-stimulated IP*x* accumulation. At the higher doses of AngII (10–100 nM), RZ5 had no effect on IP*x* accumulation. That the IP*x* signal in RGS5 ribozyme-treated cells is lower at high (10 nM) but not low (1–3 nM) AngII concentrations might be due to fast desensitization of angiotensin receptor, especially with

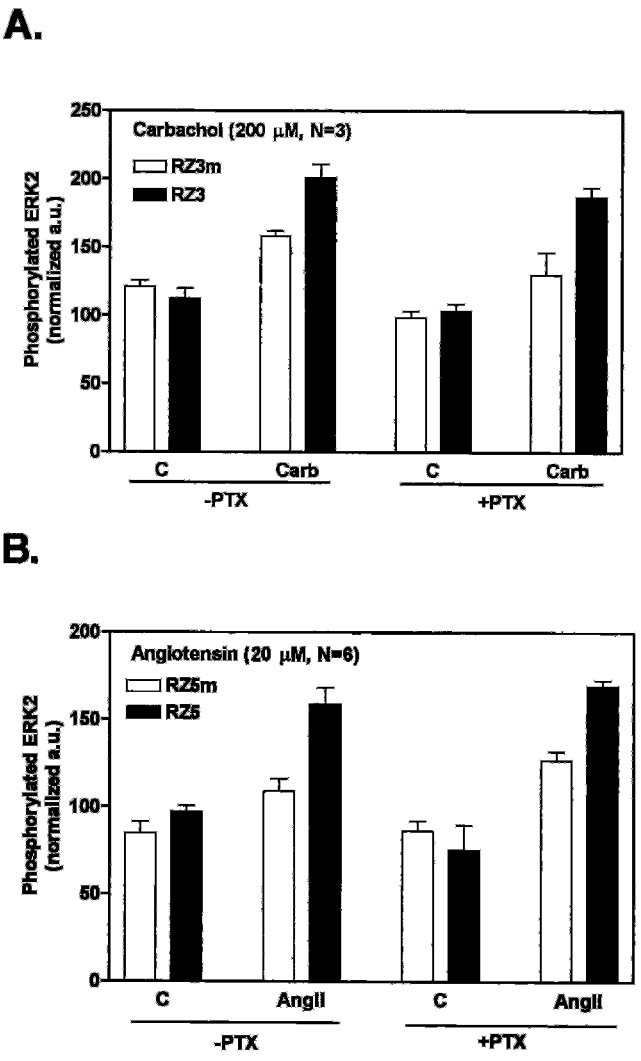

FIG. 6. **PTX insensitivity of RGS3 and RGS5 ribozyme-enhanced MAP kinase activity.** *A*, A-10 cells transfected with the inactive RGS3 ribozyme (*RZ3m*) or RGS3 ribozyme (*RZ3*) were serum-starved for 40 h as described in Fig. 5. Cultures were treated with (+*PTX*) or without (−*PTX*) 30 ng/ml pertussis toxin overnight prior to stimulation with 200 μM carbachol (*Carb*) or control with medium (*C*) for 5 min, and lysates were prepared for Western blot analysis of ERK phosphorylation. Data represent the mean ± S.E. of three independent experiments. *B*, A-10 cells were transfected with angiotensin AT1a receptor plasmid plus the inactive RGS5 ribozyme (*RZ5m*) or active RGS5 ribozyme (*RZ5*). Cells were starved for 40 h and pretreated with (+*PTX*) or without (−*PTX*) 30 ng/ml PTX overnight. At 72 h post-transfection, cells were stimulated with (*AngII*) or without (*C*) AngII (20 μM) for 5 min and harvested for Western blot analysis. Data represent the mean ± S.E. of six independent experiments.

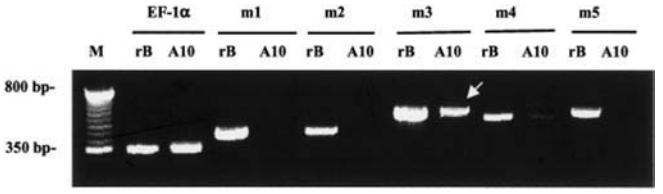

FIG. 7. **mRNA expression of muscarinic receptor subtypes in A-10 cells by RT-PCR**. Total RNA prepared from either A-10 cells (*A10*) or rat brain (*rB*, as positive control) was subjected to RT-PCR with muscarinic receptor subtype-specific primers (m1, m2, m3, m4, and m5) as described under "Experimental Procedures." Elongation factor (*EF-1α*) was amplified under identical conditions as an internal control. The PCR products were separated by 1.8% agarose gel electrophoresis and stained with ethidium bromide and photographed.

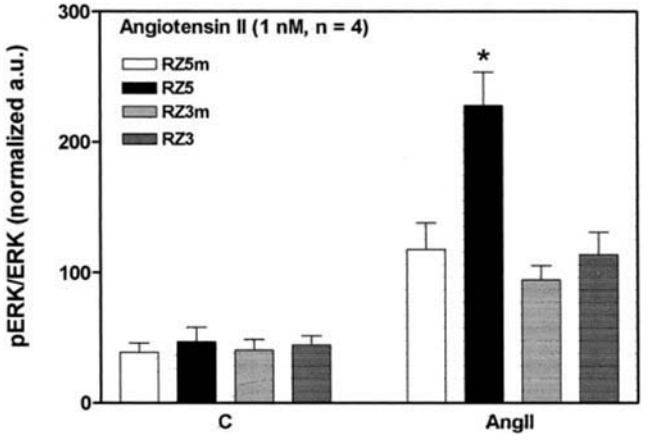

FIG. 8. **Effect of RGS5 ribozyme in enhancing AngII-stimulated MAP kinase activity in RAOSMC.** After transfection with RGS-specific ribozymes (*RZ3* and *RZ5*) or the corresponding inactive ribozymes (*RZ5m* and *RZ3m*) in RAOSMC, cells were serum-starved for 48 h prior to stimulation with 1.0 nM AngII for 5 min at 72 h post-transfection, harvested with 1× Sample Buffer, subjected to 12% SDS-PAGE, and analyzed by Western blot as described under "Experimental Procedures." Both p42 and p44 were detected and showed similar responses, so the combined densities of the 42- and 44-kDa bands were quantitated. The *graph* shows the mean ± S.E. of *pERK/ERK* for four independent experiments. The *asterisk* indicates that RGS5 ribozyme produced a statistically significant ($p < 0.01$) enhancement of AngII-stimulated MAP kinase activity (*AngII*, *black bars*) compared with AngII plus the inactive RGS5 ribozyme (*AngII*, *white bars*).

higher doses. These results further confirm the selectivity of RGS5 ribozyme for AT1aR responses and indicate that RGS5 is likely working on G_q to regulate AT1a receptor signaling.

DISCUSSION

In this study, we have used ribozyme technology to specifically suppress the expression of different RGS proteins in a rat aorta smooth muscle cell line (A-10 cells) and primary cultures of RAOSMC. Two major conclusions can be derived from this study. 1) Ribozymes can be easily designed to selectively suppress the expression of particular RGS at both the mRNA and protein levels. 2) Ribozyme-mediated suppression of RGS3 and RGS5 differentially enhances MAP kinase activity stimulated by carbachol and angiotensin II, respectively, providing novel evidence of receptor specificity of the actions of endogenous RGS3 and RGS5 protein in vascular smooth muscle cells.

Ribozymes as Tool for Studying Protein Families—There are a number of methods that can be used to assess the function of endogenous proteins such as those in the RGS family. Neutralizing antibodies have been used but are mainly applicable to electrophysiological studies because the pipette provides access to the intracellular space (24). RGS-inhibiting drugs would be useful (40) but are not yet available, certainly not with the potency or specificity required for use in defining the functions of individual RGS proteins. Thus reverse genetics approaches to suppress expression of endogenous RGS protein remain the best choice. There are now several such approaches as follows: antisense (either oligonucleotides or expressed reversed full-length constructs), ribozymes, or the recently described double-stranded RNA interference ("RNAi") method (41). To date, there are only two published reports applying these approaches to RGS proteins. These studies (17, 42) used antisense oligos and full-length antisense expression constructs to reduce expression of RGS9 and RGS3, respectively. Ribozymes, antisense oligos, and RNAi all utilize small recognition sequences (*e.g.* 15–25 bp) but require introduction into the cell. Ribozymes have two potential advantages over RNAi and antisense oligos. First, they act catalytically as site-specific ribonucleases, resulting in degradation of the targeted RNA. Second, in addition to the complementarity between the ribozyme and flanking

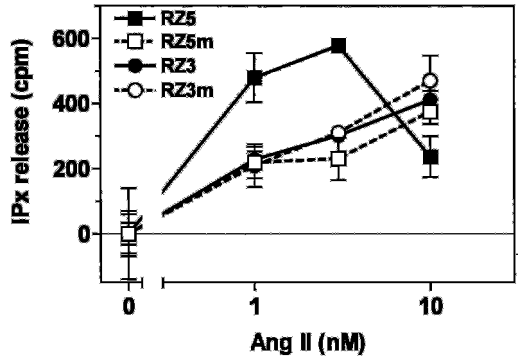

FIG. 9. **Effect of RGS5 ribozyme in enhancing angiotensin II-stimulated IP*x* accumulation in RAOSMC.** After transfection with RGS-specific ribozymes (*RZ3* and *RZ5)* or the corresponding inactive ribozymes (*RZ5m* and *RZ3m*) in RAOSMC, cells were labeled with [^{3}H]myoinositol for 24 h and incubated with the indicated concentration of AngII for 30 min. Inositol phosphates (*IPx*) were isolated and quantitated as described under "Experimental Procedures." Data are mean ± S.E. of three AngII dose-response experiments. Values for IP*x* counts in the presence of LiCl alone were subtracted from the angiotensin-stimulated IP*x* release.

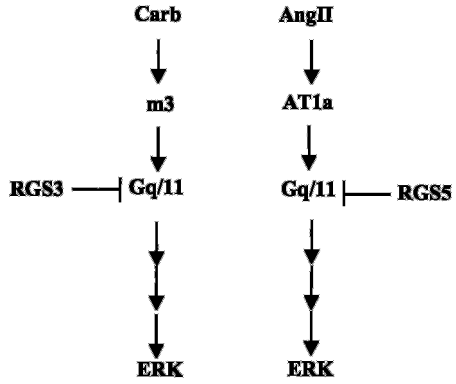

FIG. 10. **Model of receptor-selectivity of RGS3 and RGS5 proteins.**

regions on the template, ribozyme function also depends on the presence of the GUC cleavage site. Thus a partial match between the ribozyme and a target RNA would not yield effective degradation if the GUC were not present in the correct location. A potential disadvantage of ribozymes over DNA antisense oligonucleotides is the low stability of RNA in cells.

In this report, we describe the utility of a set of RGS ribozymes. To avoid the rapid degradation *in vivo* (43), we used chimeric DNA-RNA ribozymes and introduced phosphorothioate linkages at the 3′-end as reported previously (29, 44–46). The ~50% suppression of mRNA for RGS2, -3, -5, and -7 (Fig. 3, *A* and *B*), and protein for RGS3 (Fig. 4*B*) is quite substantial given our transfection efficiency of about 50%. Thus, the mRNA and protein appear to be almost completely suppressed in the transfected population of cells. This compares favorably with the recent report of RNAi-mediated inhibition in mammalian cells that showed almost 100% suppression of protein expression from a co-transfected luciferase reporter with 70–90% transfection efficiency (41). Furthermore, all four of the tested ribozymes (RZ2, -3, -5, and -7) were effective in suppressing the cognate RGS mRNA but did not suppress levels of other RGS mRNAs. Because the first ribozyme designed for each RGS worked, our findings suggest that stabilized ribozymes (*i.e.* DNA-RNA chimers with phosphorothioation) should be a simple and robust strategy for reverse genetic studies of closely related proteins in multimember families.

Role of Endogenous RGS Proteins in Specific Receptor Signaling Pathways—Very few reports exist that detail the contribution of endogenous RGS proteins to specific receptor responses. The use of RGS-insensitive G proteins (10, 47) has revealed a prominent role for endogenous RGS proteins in neuronal function *in vitro* (21, 48). This latter approach, however, blocks the function of all RGS proteins at the mutated Gα subunit and thus cannot identify which specific RGS protein(s) are involved. Two RGS "knockout" mouse strains have been reported, RGS9 (22) and RGS2 (23). The former has prominent alterations in the kinetics of the retinal photoresponse (known to be mediated by the photon-receptor rhodopsin), and the latter has immunologic and behavioral phenotypes (but the underlying receptor system(s) remain undefined). The most specific information to date has been derived from neutralizing antibody studies of DRG neuron presynaptic neurotransmitter signaling that show RGS4 and Gα interacting protein to have differential effects on α_{2A}-adrenergic receptor coupling to calcium channel inhibition (49), whereas RGS12 seems to mediate selectively the desensitization of γ-aminobutyric acid, type B–receptor responses (24).

In this report, we show that endogenous RGS3 and RGS5 in rat A-10 vascular smooth muscle cells and primary culture of aorta smooth muscle cells have selective effects on MAP kinase stimulation by muscarinic and angiotensin receptors. The observation that MAP kinase stimulation is enhanced when RGS levels are reduced suggests that there is tonic (or rapidly inducible) inhibition of these receptor responses by the endogenous RGS proteins. RGS3 has been shown previously to regulate MAP kinase responses both in overexpression and antisense knockdown studies (17). RGS5 overexpression, however, did not regulate MAP kinase activation induced by platelet-activating receptor (50). RGS5 is differentially expressed in arterial smooth muscle compared with venous smooth muscle (51). Thus the selectivity of RGS5 effects for angiotensin receptors (this paper) and platelet-activating factor receptors (50) is quite interesting in light of the limited tissue distribution of RGS5 expression.

The RGS specificity observed here could be occurring at the G protein level or may be dependent on receptor-RGS contacts (direct or indirect). The muscarinic receptor response in A-10 cells seems to be mediated by the m3 subtype given the pertussis toxin insensitivity of the response and the abundance of m3 muscarinic receptor message compared with m1 and m5 receptor transcripts. The m3 receptor is well known to activate $G_{q/11}$ (38) but has also been reported recently (51) to activate G_{12} or G_{13}. In contrast, angiotensin receptors, which strongly activate $G_{q/11}$ and G_i family members, do not appear to activate G_{12} or G_{13} (53). The pertussis toxin insensitivity strongly implicates $G_{q/11}$ for AT1a receptors, but the m3 response could be either $G_{q/11}$- or $G_{12/13}$-mediated. The former is more likely because RhoA, which is activated by $G_{12/13}$, is not considered to be directly linked to ERK activation (54), whereas $G_{q/11}$-mediated PKC activation can activate ERK by several mechanisms (55). Also RGS3 has been reported not to be a GAP for Gα_{12} (16). For angiotensin receptor (AT1a), it has been reported that it signals via both heterotrimeric G proteins ($G_{q/11}$) and non-membrane tyrosine kinases (Jak2-STAT1) pathways that can activate MAP kinase and induce IP*x* accumulation through phospholipase C activation (33, 56–58). Thus, it appears that both RGS3 and RGS5 are working through effects on G_q or G_{11} (Fig. 10), but the precise mechanism for receptor selectivity will require additional study.

Concluding Remarks—These data show that endogenous RGS3 is a negative modulator of ERK activation by endogenous muscarinic m3 receptors mediated through a non-$G_{i/o}$, probably $G_{q/11}$ pathway. At the same time, endogenous RGS5 is a negative modulator of AT1a receptor-mediated activation of ERK

through a non-$G_{i/o}$, probably $G_{q/11}$, mechanism in both A-10 cells and primary culture of aorta smooth muscle cells. Thus we demonstrate a novel receptor selectivity of RGS3 and RGS5 action in important signaling pathways in a differentiated cells from vascular smooth muscle. The degree to which this conclusion may be generalized to other signaling pathways and other cell types is unclear and will depend on the precise mechanisms that determine this selectivity. This study, however, is the first to report such a clear receptor selectivity for endogenous RGS proteins in which a given RGS preferentially regulates a given receptor and provides useful tools, the stabilized ribozymes, to permit the analysis of RGS function in a broader range of cellular functions.

REFERENCES

1. Hepler, J. R., and Gilman, A. G. (1992) *Trends Biochem. Sci.* **17,** 383–387
2. Birnbaumer, L. (1992) *Cell* **71,** 1069–1072
3. Siderovski, D. P., Strockbine, B., and Behe, C. I. (1999) *Crit. Rev. Biochem. Mol. Biol.* **34,** 215–251
4. Berman, D. M., Wilkie, T. M., and Gilman, A. G. (1996) *Cell* **86,** 445–452
5. De Vries, L., Zheng, B., Fisher, T., Elenko, E., and Farquhar, M. G. (2000) *Annu. Rev. Pharmacol. Toxicol.* **40,** 235–271
6. Ross, E. M and Wilkie, T. M. (2000) *Annu. Rev. Biochem.* **69,** 795–827
7. Zheng, B., Ma, Y. C., Ostrom, R. S., Lavoie, C., Gill, G. N., Insel, P. A., Huang, X. Y., and Farquhar, M. G. (2001) *Science* **294,** 1939–1942
8. Heximer, S. P., Watson, N., Linder, M. E., Blumer, K. J., Hepler, J. R. (1997) *Proc. Natl. Acad. Sci. U. S. A.* **94,** 14389–14393
9. Hepler, J. R., Berman, D. M., Gilman, A. G., and Kozasa, T. (1997) *Proc. Natl. Acad. Sci. U. S. A.* **94,** 428–432
10. Lan, K. L., Zhong, H., Nanamori, M., and Neubig, R. (2000) *J. Biol. Chem.* **275,** 33497–33503
11. Traver, S., Bidot, C., Spassky, N., Baltauss, T., De Tand, M. F., Thomas, J. L., Zalc, B., Janoueix-Lerosey, I., and Gunzburg, J. D. (2000) *Biochem. J.* **350,** 19–29
12. Hepler, J. R. (1992) *Trends Pharmacol. Sci.* **20**, 376–382
13. Zheng, B., De Vries, L., and Farquhar, M. G. (1999) *Trends Biochem. Sci.* **24,** 411–414
14. Seki, N., Sugano, S., Suzuki, Y., Nakagawara, A., Ohira, M., Muramatsu, M., Saito, T., and Hori, T. (1998) *Hum. Genet.* **43,** 202–205
15. Zhou, J., Moroi, K., Nishiyama, M., Usui, H., Seki, N., Ishida, J., Fukamizu, A., and Kimura, S. (2001) *Life Sci.* **68,** 1457–1469
16. Scheschonka, A., Dessauer, C. W., Sinnarajah, S., Chidiac, P., Shi, C. S., and Kehrl, J. H. (2000) *Mol. Pharmacol.* **58,** 719–728
17. Dulin, N. O., Sorokin, A., Reed, E., Elliott, S., Kehrl, J. H., and Dunn, M. J. (1999) *Mol. Cell. Biol.* **19,** 714–723
18. Neill, J. D., Duck, L. W., Sellers, J. C., Musgrove, L. C., Scheschonka, A., Druey, K. M., and Kehrl, J. N. (1997) *Endocrinology* **138,** 843–846
19. Zeng, W., Xu, X., Popov, S., Mukhopadhyay, S., Chidiac, P., Yagaloff, K. A., Fisher, S. L., Ross, E. M., Muallem, S., and Wilkie, T. M. (1998) *J. Biol. Chem.* **273,** 34687–34690
20. Snow, B. E., Hall, R. A., Krumins, A. M., Brothers, G. M., Bouchard, D., Brothers, C. A., Chung, S., Mangion, J., Gilman, A. G., Lefkowitz, R. J., and Siderovski, D. P. (1998) *J. Biol. Chem.* **273,** 17749–17755
21. Jeong, S. W., and Ikeda, S. R. (2000) *J. Neurosci.* **20,** 4489–4496
22. Chen, C. K., Burns, M. E., He, W., Wensel, T. G., Baylor, D. A., and Simon, M. I. (2000) *Nature* **403,** 557–560
23. Oliveira-dos-Santos, A. J., Matsumoto, G., Snow, B. E., Bai, D., Houston, F. P., Whishaw, I. Q., Mariathasan, S., Sasaki, T., Wakeham, A., Ohashi, P. S., Roder, J. C., Barnes, C. A., Siderovski, D. P., and Penninger, J. M. (2000) *Proc. Natl. Acad. Sci. U. S. A.* **97,** 12272–12277
24. Schiff, M. L., Siderovski, D. P., Jordan, J. D., Brothers, G., Snow, B., De Vries, L., Ortiz, D. F., and Diverse-Pierluissi, M., (2000) *Nature* **408,** 723–727
25. Alexander, R. W., and Griendling, K. K. (1996) *J. Hypertens.* **14,** S51–S54
26. Yalkinoglu, A.O., Spreyer, P., Bechem, M., Apeler, H., and Wohlfeil, S. (1995) *J. Recept. Signal. Transduct. Res.* **15,** 117–130
27. Touyz, R. M., and Schiffrin, E. L. (1996) *J. Biol. Chem.* **271,** 24353–24358
28. Benjamin, C. W., Linseman, D. A., and Jones, D. A. (1994) *J. Biol. Chem.* **269,** 31346–31349
29. Wang, Q., Mullah, B., Hansen, C., Asundi, J., and Robishaw, J. D. (1997) *J. Biol. Chem.* **272,** 26040–26048
30. Wang, Q., Jolly, J. P., Surmeier, J. D., Mullah, B., Lidow, M. S., Bergson, C. M., and Robishaw, J. D. (2001) *J. Biol. Chem.* **276**, 39386–39393
31. Grassi, G., Forlino, A., and Marini, J. C. (1997) *Nucleic Acids Res.* **25,** 3451–3458
32. Dudley, D. T., Panek, R. L., Major, T. C., Lu, G. H., Bruns, R. F., Klinkefus, B. A., Hodges, J. C., and Weishaar, R. E. (1990) *Mol. Pharmacol.* **38,** 370–377
33. Seta, K., Nanamori, M., Modral, J. G., Neubig, R. R., and Sadoshima, J. (2002) *J. Biol. Chem.* **277,** 9268–9277
34. Grant, S. L., Lassegue, B., Griendling, K. K., Ushio-Fukai, M., Lyons, P. R., and Alexander, R. W. (2000) *Mol. Pharmacol.* **57,** 460–467
35. Kardestuncer, T., Wu, H., Lim, A. L., and Neer, E. J. (1998) *FEBS Lett.* **438,** 285–288
36. Chattejee, T. K., Eapen, A. K., and Fisher, R. A. (1997) *J. Biol. Chem.* **272,** 15481–15487
37. Druey, K. M., Blumer, K. J., Kang, V. H., and Kehrl, J. U. (1996) *Nature* **379,** 742–746
38. Caulfield, M. P., and Birdsall, N. J. M., (1998) *Pharmacol. Rev.* **50,** 279–290
39. Dohlman, H. G., Song, J., Ma, D., Courchesne, W. E., and Thorner, J. (1996) *Mol. Cell. Biol.* **16,** 5194–5209
40. Zhong, H. L., and Neubig, R. R. (2001) *J. Pharmacol. Exp. Ther.* **297,** 837–845
41. Elbashir, S. M., Harborth, J., Lendeckel, W., Yalcin, A, Weber, K., and Tuschl, T. (2001) *Nature* **411,** 494–498
42. Garzon, J., Rodriguez-Diaz, M., Lopez-Fando, A., and Sanchez-Blazquez, P. (2001) *Eur. J. Neurosci.* **13,** 801–811
43. Heidenreich, O., and Eckstein, F. (1992) *J. Biol. Chem.* **267,** 1904–1909
44. Gu, J., Veerapanane, D., Rossi, J., Natarajan, R., Thomas, L., and Nadler, J. (1995) *Circ. Res.* **77**, 14–20
45. Shimayama, T., Nishikawa, F., Nishikawa, S., and Taira, K. (1993) *Nucleic Acids Res.* **21,** 2605–2611
46. Taylor, N., Kaplan, B., Swiderski, P., Haitang, L., and Rossi, J. (1992) *Nucleic Acids Res.* **20,** 4559–4565
47. DiBello, P. R., Garrison, T. R., Apanovitch, D. M., Hoffman, G., Shuey, D. J., Mason, K., Cockett, M. I., and Dohlman, H. G. (1998) *J. Biol. Chem.* **273,** 5780–5784
48. Chen, H., and Lambert, N. A. (2000) *Proc. Natl. Acad. Sci. U. S. A.* **97,** 12810–12815
49. Diverse-Pierluissi, M., Fischer, T., Jordan, J. D., Schiff, M. L., Ortiz, D. F., Farquhar, M. G., and De Vries, L. (1999) *J. Biol. Chem.* **274,** 14490–14494
50. Zhang, Y., Neo, S. Y., Han, J., Yaw, L. P., and Lin, S. C. (1999) *J. Biol. Chem.* **274,** 2851–2857
51. Adams, L. D., Geary, R. L., McManus, B., and Schawrtz, S. M. (2000) *Circ. Res.* **87,** 623–631
52. Rumenapp, U., Asmus, M., Schablowski, H., Woznicki, M., Han, L., Jakobs, K. H., Fahimi-Vahid, M., Michalek, C., Wieland, T., and Schmidt, M. (2001) *J. Biol. Chem.* **276,** 2474–2479
53. Gohla, A., Offermanns, S., Wilkie, T. M., and Schultz, G. (1999) *J. Biol. Chem.* **274**, 17901–17907
54. Whitehead, I. P., Zohn, I. E., and Der, C. J. (2001) *Oncogene* **20,** 1547–1555
55. Gutkind, J. S. (1998) *J. Biol. Chem.* **273,** 1839–1842
56. Schorb, W., Peeler, T. C., Madigan, N. N., Conrad, K. M., and Baker, K. M. (1994) *J. Biol. Chem.* **269,** 19626–19632
57. Sadoshima, J., Qiu, Z. H., Morgan, J. P., and Izumo, S. (1995) *Circ. Res.* **76,** 1–15
58. Doan, T. N., Showkat Ali, M., and Bernstein, K. E. (2001) *J. Biol. Chem.* **276,** 20954–20958